Ab Initio Study of Hydrogen-Bond Formation between Aliphatic and Phenolic Hydroxy Groups and Selected Amino Acid Side Chains

Peter I. Nagy* and Paul W. Erhardt

Center for Drug Design and Development, College of Pharmacy, The University of Toledo, Toledo, Ohio 43606-3390

Received: November 14, 2007; In Final Form: February 1, 2008

Hydrogen bonding was studied in 24 pairs of isopropyl alcohol and phenol as one partner, and water and amino-acid mimics (methanol, acetamide, neutral and protonated imidazole, protonated methylalamine, methylguanidium cation, and acetate anion) as the other partner. MP2/6-31+G* and MP2/aug-cc-pvtz calculations were conducted in the gas phase and in a model continuum dielectric environment with dielectric constant of 15.0. Structures were optimized in the gas phase with both basis sets, and zero-point energies were calculated at the MP2/6-31+G* level. At the MP2/aug-cc-pvtz level, the BSSE values from the Boys−Bernardi counterpoise calculations amount to 10−20 and 5−10% of the uncorrected binding energies of the neutral and ionic complexes, respectively. The geometry distortion energy upon hydrogen-bond formation is up to 2 kcal/mol, with the exception of the most strongly bound complexes. The BSSE-corrected MP2/aug-cc-pvtz binding energy of −27.56 kcal/mol for the gas-phase acetate···phenol system has been classified as a short and strong hydrogen bond (SSHB). The $CH_3NH_3^+$···isopropyl alcohol complex with binding energy of −22.54 kcal/mol approaches this classification. The complete basis set limit (CBS) for the binding energy was calculated for twelve and six complexes on the basis of standard and counterpoise-corrected geometry optimizations, respectively. The X···Y distances of the X−H···Y bridges differ by up to 0.03 Å as calculated by the two methods, whereas the corresponding CBS energy values differ by up to 0.03 kcal/mol. Uncorrected MP2/aug-cc-pvtz hydrogen-bonding energies are more negative by up to 0.35 kcal/mol than the MP2/CBS values, and overestimate the CCSD(T)/CBS binding energies generally by up to 5% for the eight studied complexes in the gas phase. The uncorrected MP2/aug-cc-pvtz binding energies decreased (in absolute value) by 11−18 kcal/mol for the ionic species and by up to 5 kcal/mol for the neutral complexes when the electrostatic effect of a polarizable model environment was considered. The $\Delta E^{CCSD(T)} - \Delta E^{MP2}$ corrections still remained close to their gas-phase values for four complexes with 0, ±1 net charges. Good correlations ($R^2 = 0.918-0.958$) for the in-environment MP2/aug-cc-pvtz and MP2/6-31+G* hydrogen-bonding energies facilitate the high-level prediction of these energies on the basis of relatively simple MP2/6-31+G* calculations.

Introduction

Theoretical characterization of the interactions and chemical transformations in biological systems is a rapidly developing area of computational chemistry. For systems sometimes having thousands of atoms, only molecular-mechanics-based methods become practical. However, these methods cannot handle transformations involving breaking and making chemical bonds. Quantum-chemical methods, useful in these cases, have severe limitations upon the size of the system. Energies/free energies calculated by utilizing semiempirical quantum-chemical methods may not reach the precision required for providing valuable support for theory-based drug design. High-level theoretical calculations are affordable today only on fairly small systems or on models for larger systems. This latter approach has been applied in the present study.

One of the major stabilizing factors in biological systems is the hydrogen bond[1] formed within biopolymers and between the macromolecule and a ligand. Proper estimation of the latter interaction is of central importance in drug design. In proteins, the polar site of the amino acid residue side chain is connected to the backbone through at least one $-CH_2-$ group. Hydrogen-bonded complexes with protein mimics, where the aliphatic part of the residue side chain has been replaced with a methyl group (or simply with a hydrogen in the imidazole complexes), may successfully model the original systems, because hydrogen-bond energies are primarily independent of the length and the conformation of the side chain.

In many cases, the ligand has two (or more) polar sites and is capable of forming more than one hydrogen bond with the protein. In such cases, it is crucial to explore which combination of hydrogen bonds comes into existence, because this can dictate the orientation of the ligand at the binding site. The structures of the isomeric hydrogen-bonded systems may primarily modify the biological response triggered by the actual mode of how the ligand has bound to the protein. An example of high interest is the activation of the human estrogen receptor (hER).

It is commonly accepted that precise spacing between two OH groups separated by an essentially planar and fairly hydrophobic scaffold are the main structural features for ligand binding with the hER.[2] The natural agonist at the hER is the human hormone 17β-estradiol. In the binding model of Tanenbaum et al.,[3] the phenolic OH-group of 17β-estradiol is a hydrogen bond donor to the Glu353 carboxylate while also serving as an acceptor for hydrogen bonds with a nearby water and the protonated Arg394. The 17-aliphatic OH interacts with the imidazole system in His524.

* Corresponding author. E-mail: pnagy@utnet.utoledo.edu.

10.1021/jp7108847 CCC: $40.75
Published on Web 03/29/2008

There is growing evidence that some natural and non-natural chemicals have the potential to disrupt the human endocrine system by mimicking endogenous hormones, such as the androgens and estrogens.[4] Among others, natural products found in soybean, e.g., genistein and glyceollins, may have estrogen activity.[5,6] These polycyclic systems contain two oxygen atoms (two phenolic OH groups, or a cyclic ether and a phenolic OH) at the required separation for possible binding to hER. Simple molecular mechanics geometry optimization suggests that the crucial oxygen atoms nearly overlap with those in 17β-estradiol when the structures are superimposed. Because the oxygen atoms at either end of these polycyclic natural products are capable of interacting with either of the two hER binding sites, two distinct orientations become possible during binding. It is generally not clear which of these orientations will be preferred within the hER binding cavity. Recently, the binding energies between cyclic ethers and protein mimics were calculated, where the cyclic ethers served as models for the ether sites of glyceollins.[7] In the present study, the hydrogen bond energies have been calculated for model complexes having different protein side-chain mimics as one partner, and i-propanol or phenol as the other partner. The latter two molecules serve as estradiol mimics.

As mentioned above, theoretical prediction of protein−ligand hydrogen-bond energies can be extremely important during drug design. For practical reasons, however, only relatively low-level computations can be applied to large molecular complexes. One of the goals in the present study was to examine correlations between high and lower-level energy values in order to predict the hydrogen-bond energies based on calculations performed at the more practical MP2/6-31+G* level. The theoretical investigations described herein include standard and counterpoise-corrected geometry optimizations for the complexes up to the MP2/aug-cc-pvtz level. Calculated binding energies have been corrected for the basis set superposition error. For several complexes, the complete basis set (CBS) limit, $MP2_{CBS}$ for the binding energy has also been determined.

Correlation effects may not be negligible beyond the MP2 level. In a recent review, Hobza[1f] proposed a formula for calculating the hydrogen-bonding energies at the CCSD(T) level at the CBS limit as follows

$$\Delta E^{CCSD(T)}{}_{CBS} = \Delta E^{MP2}{}_{CBS} + (\Delta E^{CCSD(T)}{}_{sb} - \Delta E^{MP2}{}_{sb}) \quad (1)$$

Here the subscript "sb" refers to calculations performed with a relatively small basis set. Equation 1 is based on the assumption that the correction term (in parentheses) to the MP2/CBS limit of the binding energy, $\Delta E^{MP2}{}_{CBS}$, is of small basis set dependency. Indeed, the correction term for a few complexes becomes nearly constant when calculated with basis sets of at least cc-pvdz quality.[1f] In our study, this term has been estimated at the aug-cc-pvdz level or higher.

Hydrogen-bond energies calculated in the gas phase may be remarkably different from those calculated in a condensed phase. Because our intention is to use the obtained values for characterizing the strength of binding in protein−ligand complexes from electrostatic point of view, the polarization upon the protein environment must also be considered. To address this effect, we performed calculations to assess changes in hydrogen-bond energies based on an environment modeled by a polarizable continuum with a dielectric constant of 15.0.

Methods and Calculations

Hydrogen bonds for i-propanol (isopropyl alcohol) and phenol have been studied across seven amino acid side-chain mimics:

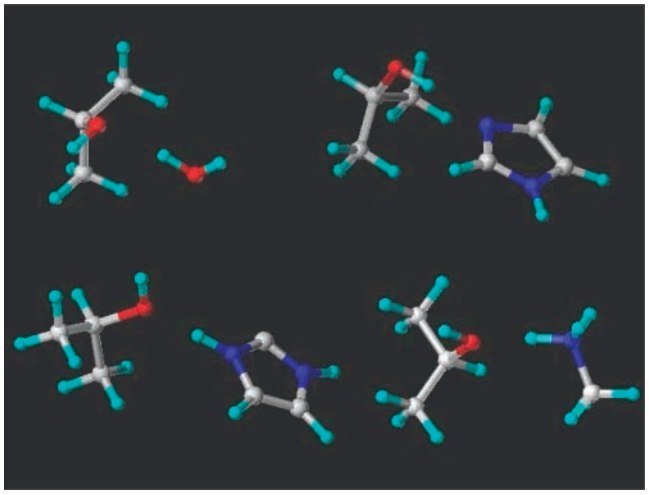

Figure 1. MP2/aug-cc-pvtz optimized geometries in the gas phase for (a) water(donor)···i-propanol(acceptor) (upper left), (b) i-propanol-(donor, trans OH)··· imidazole(acceptor) (upper right), (c) imidazoleH^+-(donor)···i-propanol(acceptor) (lower left), and (d) $CH_3NH_3^+$(donor)···i-propanol(acceptor, trans OH) (lower right) complexes. Color code: C (white), H (cyan), O (red), N (blue).

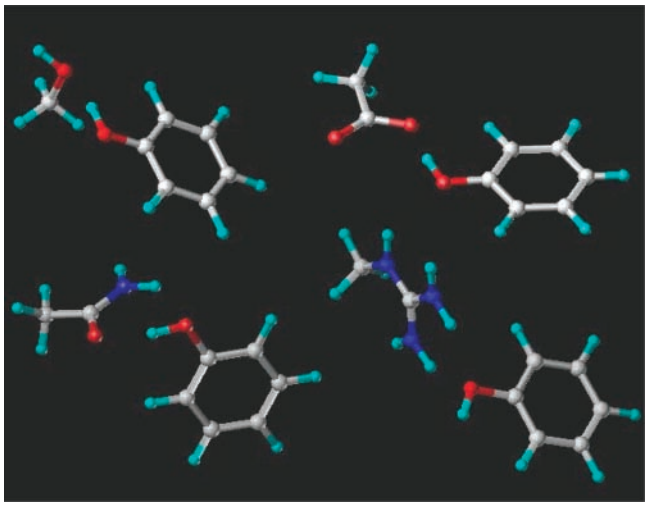

Figure 2. MP2/aug-cc-pvtz optimized geometries in the gas phase for (a) phenol(donor)···CH_3OH(acceptor) (upper left), (b) phenol-(donor)···CH_3COO^-(acceptor) (upper right), (c) phenol(donor/acceptor)··· CH_3CONH_2 (acceptor/donor) (lower left), and (d) CH_3GuaH^+(donor)···phenol (acceptor) (lower right) complexes. For color code, see Figure 1.

(i) CH_3OH (mimic for serine and threonine); (ii and iii) neutral and protonated imidazole (mimics for histidine); (iv) CH_3CONH_2 (mimic for asparagine and glutamine); (v) $CH_3NH_3^+$ (mimic for protonated lysine); (vi) methyl-guanidium cation (mimic for protonated arginine); and (vii) CH_3COO^- (mimic for anionic aspartic and glutamic acids). In complexes with the protonated imidazole, $CH_3NH_3^+$, and methyl-guanidium cation, the protein mimic acted as the hydrogen-bond donor. The protein mimics acted as hydrogen-bond acceptors in complexes with CH_3COO^- and CH_3CONH_2. Finally, in the complexes of CH_3OH or imidazole with i-propanol or phenol, each component acted both as proton donor and acceptor. Accordingly, altogether 18 pairs of complexes have been studied. Optimized geometries for selected complexes are shown in Figures 1 and 2.

Because water molecules may also participate during ligand binding, interactions of i-propanol and phenol with water have also been considered. In the case of i-propanol, both the gauche and trans conformations of the alcoholic hydrogen in the H−C−

O−H moiety were studied. Water was treated as both a hydrogen-bond donor and an acceptor in these six complexes.

Most studies were performed at the ab initio MP2 level.[8,9] Geometries were optimized throughout the standard procedure at the MP2/6-31+G* level and reoptimized by utilizing the aug-cc-pvtz basis set.[10] Local energy-minimum characters were certified by frequency analysis from the MP2/6-31+G* calculations. For determining the CBS limit values, binding energies were also determined after geometry optimizations at the MP2/aug-cc-pvdz level. For eight gas-phase complexes, the $\Delta E^{\mathrm{CCSD(T)}}{}_{\mathrm{CBS}}$ values were estimated on the basis of eq 1.

When the binding energies are to be determined for van der Waals complexes, a recurring problem is the role of the basis set superposition error.[11] The classical correction procedure for this error is the Boys−Bernardi method,[12] where instead of calculating the $\Delta E^{\mathrm{uncor}}$, uncorrected binding energy as

$$\Delta E^{\mathrm{uncor}} = E(\mathrm{complex}) - E(\mathrm{A})^m - E(\mathrm{B})^m \qquad (2)$$

the relevant binding energy, ΔE^{CP}, is calculated in the so-called counterpoise procedure as

$$\Delta E^{\mathrm{CP}} = E(\mathrm{complex}) - E(\mathrm{A})^d - E(\mathrm{B})^d \qquad (3)$$

E(complex) stands for the energy of the hydrogen-bonded complex in eqs 2 and 3, and $E(\mathrm{X})^m$ and $E(\mathrm{X})^d$ (X = A, B) stand for the energies of the component molecules in the monomer and dimer basis sets, respectively. To minimize the total energy of the complex, the geometries of the elements undergo changes compared to their separately optimized forms, leading to a necessary increase in their energy. Thus, the corresponding geometries for the elements as monomers, optimized in the monomer basis set, differ from that obtained throughout the optimization of the complex utilizing the dimer basis set. In a seven-point calculation for a complex, Nagy et al.[13] defined the BSSE devoid of the geometry distortion energy, GEOM, as

$$\Delta E^{\mathrm{cor}} \equiv \Delta E^{\mathrm{uncor}} - \mathrm{BSSE} = \Delta\mathrm{CP} + \mathrm{GEOM} \qquad (4)$$

GEOM is always a positive energy term.[14] BSSE, however, is of negative sign because the larger basis set used in calculations for the complex allows a more adequate description of the electron distribution for each component of the hydrogen-bonded system, and the resulting energy lowers.

As is generally accepted, the BSSE causes a nonphysical stabilization for the calculated binding energy. Furthermore, the question may be raised whether the BSSE affects only the energy results or has an effect on the optimized geometry as well. Simon et al.[15] performed geometry optimizations for small hydrogen-bonded complexes where the BSSE was considered in every step of the procedure (counterpoise-corrected (CP) optimization). These authors found that the CP geometry optimization led to larger heavy atom separation in the X−H···Y bond than with the standard procedure when the 6-31G-(d,p) and the D95 ++(d,p) basis sets were used at the HF and MP2 levels. Hobza and Havlas[16] have also argued in favor of the CP optimization because the standard optimization failed to find a stationary point for the quasi-linear structure of the HF dimer at the MP2/6-31G** level. In contrast, Halkier et al.[17] noticed a rapid convergence of the MP2/CP optimized O...O equilibrium separation to the MP2/non-CP (standard) optimized value with basis sets aug-cc-pvXz, X = D, T, Q for the water dimer, and the calculated BSSE values were small with large basis sets. In our recent study,[7] differences in the (O)H···O and (N)H···O distances of 0.020−0.034 and 0.020 Å, respectively, were calculated at the MP2/aug-cc-pvtz level when the standard and CP geometry optimizations were applied for the water dimer and for the CH_3OH···oxocyclobutane and $CH_3NH_3^+$···oxocyclobutane complexes. Despite these differences in the system geometries, neither the uncorrected nor the BSSE-corrected binding energies differed by more than 0.03 kcal/mol. On the basis of these results, the standard geometry optimization was generally used in the present study.

An alternative to the BSSE correction for the binding energy is when the binding energy is calculated by eq 2, but the energy for each element has been extrapolated to the complete basis set (CBS) limit value. Wilson and Dunning[18a] and Helgaker et al.[18b] proposed inverse power formulas for the extrapolation to the CBS energy. The simplest formula applied for MP2 calculations is

$$E(\mathrm{X}) = E(\mathrm{CBS}) + A/X^3 \qquad (5)$$

where X is the so-called cardinal number in the Dunning basis-set. Following the procedure by Grabowski et al.,[19] the two parameters of eq 5 (E(CBS) and A) were calculated for selected pairs upon MP2/aug-cc-pvdz and MP2/aug-cc-pvtz calculations with X values of 2 and 3, respectively.

Having determined the $\Delta E^{\mathrm{MP2}}{}_{\mathrm{CBS}}$ values, the CBS limit of the hydrogen-bond energy at the CCSD(T) level[20] (coupled cluster with iteratively determined single and double excitations and triple excitations upon fourth-order perturbation theory), $\Delta E^{\mathrm{CCSD(T)}}{}_{\mathrm{CBS}}$, was estimated upon eq 1 for eight selected complexes. The aug-cc-pvdz basis set was applied for calculating the $\Delta E^{\mathrm{CCSD(T)}} - \Delta E^{\mathrm{MP2}}$ term for each system. To study the basis-set dependence of this CBS correction, calculations utilizing the aug-cc-pvtz basis set were also performed for the water−i-propanol and methanol−oxocyclobutene complexes in the gas phase.

In a recent review,[1g] Grabowski summarized the characteristics of short, strong hydrogen bonds. An important feature of this binding is the remarkable charge transfer, 0.1−0.4 atomic charge units from the acceptor to the hydrogen-bond donor molecule. The transferred charges have been calculated in the present study using the Mulliken population analysis and the CHELPG (grid-oriented charges from electrostatic potential) derivation method.[21]

When hydrogen bonds created between a protein and a ligand are studied, the polarization effect of the protein environment and the surrounding water molecules is not negligible. Because of the rapidly changing electric field within a protein, consideration of the environmental effect is difficult by using molecular-mechanics force-fields without including an explicit term for the polarization. A simple approach for implicit consideration of the solvent/environmental effect is the application of a distance dependent dielectric constant, ϵ. For example, the default form in the Sybyl molecular modeling package[22] is $\epsilon = 4r$. By assuming a distance of 3.5−4.0 Å for two close, nonbonded O, N, C atoms, the actual value of the dielectric constant scaling the Coulomb interaction for the two atoms is 14−16. This situation was modeled in the present study by considering a continuum dielectric environment. The IEF-PCM approach (integral-equation formalism for the polarizable continuum method[23,24]) was applied with a model-acetone solvent, whose dielectric constant was set to $\epsilon = 15$. The MP2/6-31+G* and MP2/aug-cc-pvtz geometries optimized in the gas phase were applied for the monomers and dimers. The cavity in the continuum environment was defined by overlapping spheres around the atomic centers, utilizing the Bondi radii[25] multiplied by a scaling factor of 1.2.[26] The internal energy, E_{int} and the electrostatic component of the ligand-environment

interaction, E_{elst} were calculated as

$$E_{int} = \langle \Psi | \, H \, | \Psi \rangle \quad (6a)$$

$$E_{elst} = \langle \Psi | 1/2V | \Psi \rangle \quad (6b)$$

wherein H is the system Hamiltonian, V is the reaction-field operator established in the SCF process, and Ψ is the converged wave function. It was assumed in the present study that the ligand has enough space at the receptor site, thus the free energy associated with the cavity formation should not be considered. However, the contribution of the polar sites to the total surface exposed to the environment varies upon hydrogen-bond formation even in an available cavity. In the applied approach, the change in the dispersion−repulsion interaction free energy, ΔG_{dr}, is related to the change of the total exposed surface and provides an additive term to the interaction free energy. Thus, this contribution does not depend directly on the considered theoretical level and was disregarded when the correlation of the MP2/aug-cc-pvtz and MP2/6-31+G* binding energies was calculated. The change in the dispersion−repulsion energy is mainly due to the reduced surface contribution of the polar sites, which become embedded in the hydrogen-bonded complex. Thus, ΔG_{dr} depends indirectly on the applied theoretical method through the optimized geometry. Since the aim in this part of our studies was to explore the changes in the hydrogen-bond energies upon the polarization by the environment, single-point calculations at the gas-phase optimized geometries were performed to avoid the combination of the polarization and the re-optimization effects. As a consequence, the calculated ΔG_{dr} values depend on the differences in the gas-phase geometries optimized at different levels. Table 1 shows that the O···H distances differ the most for the CH_3COO^-···phenol and the imidazole···phenol(acceptor) complexes, as calculated with the 6-31+G* and aug-cc-pvtz basis sets. The contribution of the polar sites to the exposed surface changes slightly in both cases. The (C)OO^-···HO-(phenyl) surface fraction is 14.0 and 12.8% in the 6-31+G* and aug-cc-pvtz structures, respectively. For the imidazole···phenol complex, there is practically no surface contribution due to the N−H site at either level. The OH contribution is 6.1 and 7%, respectively. Overall, the gas-phase hydrogen-bonding energies have been compared with the change of the system energy after considering the electrostatic effect of the environment at the IEF-PCM/MP2 level using the 6-31+G* and aug-cc-pvtz basis sets. For four complexes with 0, ±1 net charges, the $\Delta E^{CCSD(T)} - \Delta E^{MP2}$ corrections and the $\Delta E^{CCSD(T)}{}_{CBS}$ energies were calculated in the applied model environment. All calculations were performed by the Gaussian 03 package[27] implemented at the Ohio Supercomputer Center.

Results and Discussions

Effect of the i-Propanol Conformation. The H−C−O−H moiety in i-propanol can assume two stable conformations, namely, gauche and trans. In the gas phase, the gauche structure was calculated to be lower in energy than the trans form by 0.35 and 0.44 kcal/mol using the aug-cc-pvtz and the 6-31+G* basis sets, respectively. The most stable structure for a hydrogen-bonded system can be easily formed in cases of small molecules. When the interactions of the polar sites are considered for protein−protein or protein−ligand systems, the positions of the involved heavy atoms may become fixed by the overall favorable orientations of the constituents. Thus, hydrogen-bond donation by a secondary alcohol group may be most feasible from one of its main conformations. Supporting this scheme, it can be noted that within the hERα-17β-estradiol complex, the 17-OH group can favorably act as a hydrogen-bond donor to the imidazole nitrogen of the nearby 524 His only when in its gauche conformation. To gain further insight for the i-propanol conformations' effect upon the binding energy, we studied the hydrogen-bonded complexes of water with both the gauche and trans i-propanol.

TABLE 1. Geometric Parameters for Hydrogen-Bonded Complexes Obtained through Non-CP Optimization at the Ab Initio MP2/aug-cc-pvtz and MP2/6-31+G* Levels in the Gas Phase[a]

	i-propanol (acceptor)		phenol (acceptor)	
	O···H	O···H−X	O···H	O···H−X
CH_3OH	1.866	165.7[b]	1.991	159.9
	1.870	169.7[b]	1.969	165.5
imidazole	1.879	169.0	2.117	157.9
	1.889	175.0	1.995	161.9
$CH_3NH_3^+$	1.598	174.0[b]	1.745	162.7
	1.671	175.5[b]	1.747	164.4
imidazoleH^+	1.602	179.0	1.822	160.7
	1.670	179.1	1.797	161.8
CH_3GuaH^+[c]	1.922	149.1	1.970	148.2
	1.955	147.4	1.997	146.8
	1.946	149.4	1.969	149.1
	1.978	148.3	2.032	146.5
water	1.890	165.4	1.969	162.9
	1.887	168.6	1.969	164.4
	1.875	163.5[b]		
	1.879	167.8[b]		
	i-propanol (donor)		phenol (donor)	
	X···H	X···H−O	X···H	X···H−O
CH_3OH	1.893	168.7	1.821	163.5
	1.888	173.9	1.839	165.7
imidazole	1.912	173.9[b]	1.814	165.7
	1.954	176.7[b]	1.878	163.4
CH_3CONH_2				
=O···H−O	1.853	154.1	1.757	158.4
	1.919	150.7	1.844	152.3
N−H···O	2.004	140.3	2.137	135.0
	2.017	141.7	2.146	135.8
CH_3COO^-	1.660	177.8	1.487	171.9
	1.741	175.7	1.591	169.2
water	1.950	178.5	1.863	176.0
	1.928	178.5	1.870	177.5
	1.960	179.8[b]		
	1.933	178.4[b]		

[a] Distances in Å, angles in deg. X = O or N corresponding to the heavy atom of the partner molecule in the hydrogen bond. Upper and lower values from MP2/ aug-cc-pvtz and MP2/6-31+G* optimizations, respectively. The H−O−C−H moiety for i-propanol is in gauche position except for the indicated structures. One set with a planar phenol. [b] Trans H−C−O−H in i-propanol. [c] Double data sets because of the bifurcated hydrogen bonds obtained with both basis sets.

The corresponding data do not indicate remarkable differences at the MP2/aug-cc-pvtz level either in Table 1 or in Table 2. The hydrogen-bond geometric parameters are close to each other either with a gauche or a trans i-propanol in the complex. The BSSE corrected binding energies, ΔE^{cor} (eq 3), differ by only up to 0.07 kcal/mol. This preliminary study suggests that the conformation of the H−C−O−H moiety in i-propanol has a small effect on the calculated binding energy. The i-propanol molecule is, however, only a model of the chemical environment of the 17-OH group in a steroid molecule. In this or similar ligands, the overall chemical environment of the OH group is asymmetric and the conformation preference for the alcoholic hydrogen may differ from that in i-propanol. As mentioned above, our ultimate goal in the present study is to find correlations between energy values calculated at high and lower-levels of theory. A more balanced statistics may be obtained if

TABLE 2. Uncorrected and BSSE-Corrected Binding Energies in the Gas Phase from Ab Initio MP2/aug-cc-pvtz and MP2/6-31+G* Calculations upon Non-CP Geometry Optimization[a]

	i-propanol (acceptor)		phenol(acceptor)	
	ΔE^{uncor}	ΔE^{cor}	ΔE^{uncor}	ΔE^{cor}
CH_3OH	−7.22	−6.34[b]	−6.11	−5.00
	−8.47	−5.75[b]	−7.07	−3.79
imidazole	−8.95	−7.66	−8.32	−6.53
	−9.73	−6.97	−9.12	−5.22
$CH_3NH_3^+$	−23.55	−22.54[b]	−21.12	−19.50
	−23.91	−21.39[b]	−21.51	−17.96
imidazoleH$^+$	−21.55	−20.18	−19.77	−17.62
	−22.15	−19.05	−20.29	−15.90
CH_3GuaH^+	−21.34	−19.96	−17.49	−15.97
	−22.33	−18.81	−18.92	−15.11
water	−6.99	−6.19	−5.09	−4.36
	−8.20	−5.70	−6.22	−4.08
	−6.99	−6.26[b]		
	−8.25	−5.87[b]		
	i-propanol (donor)		phenol(donor)	
CH_3OH	−6.67	−5.80	−9.11	−7.95
	−7.96	−5.22	−10.55	−7.17
imidazole	−9.21	−8.00[b]	−12.30	−10.89
	−9.71	−6.81[b]	−12.96	−9.36
CH_3CONH_2	−11.40	−10.14	−13.28	−11.73
	−11.70	−8.80	−13.70	−9.81
CH_3COO^-	−21.53	−20.17	−29.10	−27.56
	−21.61	−18.42	−28.49	−25.21
water	−5.40	−4.78	−7.31	−6.56
	−7.06	−4.60	−9.30	−6.38
	−5.45	−4.82[b]		
	−7.05	−4.57[b]		

[a] Energies in kcal/mol. $\Delta E^{cor} = \Delta E^{uncor}$ − BSSE. Upper and lower values from MP2/aug-cc-pvtz and MP2/6-31+G* calculations, respectively. The H−O−C−H moiety is in gauche conformation in i-propanol, with the exception of the indicated water complexes, where the conformation is trans. [b] Trans H−O−C−H moiety in i-propanol.

complexes with trans i-propanol are also considered. To this aim, in some complexes with methanol, imidazole, and $CH_3NH_3^+$, the trans H−C−O−H moiety was assumed. (The trans conformation for the alcoholic hydroxy group is noted in the tables.)

Geometries. The two main geometric parameters of the hydrogen bond, the X···H distance and the X···H−Y bond angle (X, Y = O, N) are compared in Table 1, as calculated by the standard (non-CP) geometry optimization in the gas phase. In accord with the calculated binding energies in Table 2, the equilibrium separations also suggest that phenol acts as a stronger hydrogen-bond donor and a weaker acceptor than i-propanol. When the hydroxy group acts as an acceptor, the X···H separations are shorter in complexes with i-propanol than with phenol. The difference may be as large as 0.1−0.2 Å, both with neutral and protonated partners at the MP2/aug-cc-pvtz level (upper-row set). Using the 6-31+G* basis set (lower-row set), the trend is maintained, but the differences in the X···H separations are generally decreased.

In contrast, the deviations of the corresponding X···H−Y angles calculated with the two basis sets are moderate, up to 6°. With an acceptor hydroxy group, the aug-cc-pvtz X···H−Y angles are in the range of 164−179° in the i-propanol complexes (Figure 1), whereas this range is 158−163° with an acceptor phenol component. The X···H−Y bond angle is special with the CH_3GuaH^+ molecule (Figure 2), where a bifurcated hydrogen bond comes into existence for both i-propanol and phenol. The calculated angle, using any basis set and acceptor, falls in the narrow range of 146−150°. This feature of the hydrogen-bond formation with a CH_3GuaH^+ partner has also been found previously in cases for cyclic ethers.[7]

The X···H distances become smaller with a phenol partner when the hydroxy group is the hydrogen bond donor. Although the N−H···O distance with the CH_3CONH_2 partner is indicated in the lower part of the table, the hydroxy group acts as an acceptor in this hydrogen bond, thus the longer separation from the phenolic than the alcoholic oxygen is in accord with those discussed above. The difference in the X···H separation is generally up to 0.1 Å in this series. In the case of the CH_3COO^- ion, however, a difference of 0.17 Å was calculated when the aug-cc-pvtz basis set was applied. To reach the very short O···H distance of 1.487 Å with the phenol partner, the O−H bond in phenol was stretched by 0.066 Å. The O···H separation is only 1.660 Å with an i-propanol partner, suggesting considerably reduced capacity of this molecule compared to phenol for hydrogen donation. The basis set effect on the X···H distance is up to 0.1 Å for this series, as well. The hydrogen bonds are similarly bent in most cases. The largest departures from a linear hydrogen bond were consistently calculated for the complexes with the CH_3CONH_2 partner (Figure 2). In this case, however, a six-member ring was calculated including two hydrogen bonds of ═O···H−O and N−H···O.

In complexes with water, both parties can act as either hydrogen bond donor or acceptor. Water is a preferable donor to i-propanol and acceptor with phenol. The H···O separations are shorter by 0.06 − 0.09 Å in the (HO)−H···O(i-propanol) complexes than in the O(water)···H−O(i-propanol) systems at the MP2/aug-cc-pvtz level. (The plural refers to the gauche and trans conformations of i-propanol). With phenol, the separation is shorter by 0.1 Å when phenol is the donor component. In all water complexes, regardless of the partner, the O···H−O angle is 163−165° and 176−180°, when the water is the donor and the acceptor, respectively.

Effects of the CP optimization have been studied for six complexes, applying both the aug-cc-pvdz and the aug-cc-pvtz basis sets (Tables 3and 4). Table 4 includes geometries for hydrogen-bonded complexes with cyclic ethers as well, investigated by us only at the aug-cc-pvtz level previously. As found in former studies,[7,15,17] the optimized X···H(Y) and X···Y (X, Y = O and/or N) separations are larger upon CP than standard geometry optimization. The difference is quite remarkable when the aug-cc-pvdz basis is used, but decreases to 0.01−0.03 Å on the basis of the MP2/aug-cc-pvtz calculations. It is worth mentioning that the complexes were selected for testing the effects of the CP optimization on neutral, as well as positively and negatively charged hydrogen-bonded complexes. The results suggest that the differences in the calculated geometries are small when the aug-cc-pvtz basis set is used. Our computer resources did not allow for studying the selected systems with larger basis sets (aug-cc-pvqz or larger), but the calculated geometric parameters support the conclusion of Halkier et al.[17] about the rapid convergence of the MP2/CP and MP2/non-CP optimized equilibrium separation of the heavy atoms involved in a hydrogen bond when the basis sets aug-cc-pvXz, X = D, T, Q are applied. Halkier et al.[17] performed the calculations for the water dimer compared to larger complexes in the present study.

The usefulness of the specific geometry optimization can be decided only on the basis of a comparison with experimental results. For complexes in the present study, experimental structure has been found only for the phenol···water system. The structure was determined on the basis of microwave[28a] and high-resolution UV spectroscopy.[28b] The two studies provide,

TABLE 3. Optimized Geometries for Phenol, Water, and the Phenol···Water Complex and the Calculated Binding Energies with Different Optimization Methods and Basis Sets in the Gas Phase[a]

	non-CP opt		CP opt		
	aug-cc-pvdz	aug-cc-pvtz	aug-cc-pvdz	aug-cc-pvtz	exp
phenol					
O−H	0.9680	0.9641			0.9574[b]
C−O	1.3815	1.3701			1.3745
COH	108.61	108.66			108.77
CCO	116.90	117.13			117.01
water					
O−H	0.9659	0.9614			0.957[c]
HOH	103.87	104.12			104.52
phenol(donor)···water					
phenol					
O−H	0.9768	0.9729	0.9757	0.9726	
C−O	1.3747	1.3627	1.3751	1.3629	
COH	109.08	109.30	109.23	109.38	
CCO	117.32	117.56	117.24	117.51	
water					
O−H	0.9668	0.9626	0.9670	0.9625	
HOH	104.50	104.81	104.46	104.80	
intermolecular					
O···O_w	2.8440	2.8347	2.9011	2.8604	2.86[d], 2.93[e]
H···O_w	1.8679	1.8633	1.9274	1.8897	
O−H···O_w	177.43	175.99	175.44	175.61	
H−O···O_w	1.69	2.63	3.03	2.90	6.7[e]
C−O···O_w	110.77	111.93	112.26	112.27	114.8[d]
					115.5[e]
O···O_w−X[f]	134.20	133.56	132.41	134.63	137.9−138.9[d]
					144.5[e]

[a] Distances in Å, angles in deg. Optimizations were performed with the aug-cc-pvdz and aug-cc-pvtz basis sets. [b] See ref 29. [c] See ref 30. [d] See ref 28a. [e] See ref 28b. [f] X is the bisector of the H−O−H angle.

TABLE 4. Optimized Intermolecular Geometric Parameters for Hydrogen-Bonded Complexes Obtained with Different Optimization Methods and Basis Sets in the Gas Phase[a]

	non-CP opt		CP opt	
	aug-cc-pvdz	aug-cc-pvtz	aug-cc-pvdz	aug-cc-pvtz
i-propanol(donor)···water				
O···O_w	2.922	2.919	2.992	2.945
H···O_w	1.949	1.950	2.020	1.977
O−H···O_w	178.5	178.5	178.1	178.1
i-propanol···$CH_3NH_3^+$[b]				
O···N	2.662	2.655	2.700	2.671
O···H(N)	1.600	1.598	1.643	1.616
O···H−N	173.8	174.0	173.2	173.7
i-propanol···CH_3COO^-				
O···O_{ac}	2.678	2.661	2.716	2.683
H···O_{ac}	1.675	1.660	1.716	1.683
O−H···O_{ac}	176.7	177.8	178.5	178.4
CH_3OH···.oxocyclobutane[c]				
O···O_{ether}	2.763	2.759	2.825	2.787
H···O_{ether}	1.817	1.819	1.883	1.853
O−H···O_{ether}	161.8	161.3	161.3	160.1
$CH_3NH_3^+$···oxocyclobutane[c]				
N···O_{ether}	2.635	2.634	2.676	2.651
H···O_{ether}	1.568	1.570	1.615	1.590
N−H···O_{ether}	170.6	172.7	171.3	172.2

[a] Distances in Å, angles in deg. [b] Trans H−O−C−H moiety in i-propanol. [c] Aug-cc-pvtz values from ref 7.

however, fairly different values for the O···O separations of about 2.86 and 2.93 Å, respectively. The experimental structure was derived by accepting that neither the phenol nor the water geometry changes upon the formation of the complex.

Table 3 shows that some major calculated geometric parameters for the isolated phenol and water molecules agree with the experimental values within 0.0064 Å and 0.4°. Upon formation of the complex, the O−H and C−O bonds of phenol increases by about 0.009 Å and decreases by 0.007 Å, respectively, whereas the bond angles change by up to 0.7°. An increase in the X−H bond length of the donor molecule in a hydrogen-bonded system has been generally found for the complexes in this study. The increase is moderate for neutral complexes but may reach 0.066 Å in negatively charged complexes (see above), or 0.047 Å for the $CH_3NH_3^+$···oxocyclobutane complex.[7] It is not obvious to us whether consideration of the calculated geometric changes for the phenol···water complex would remarkably affect the

TABLE 5. ΔE^{MP2} and Complete Basis Set Limit Values $\Delta E^{MP2}{}_{CBS}$ of the Interaction Energies for Selected Hydrogen-Bonded Complexes as Calculated with Different Optimization Methods in the GasPhase[a]

	non-CP opt			CP opt		
	aug-cc-pvdz	aug-cc-pvtz	CBS	aug-cc-pvdz	aug-cc-pvtz	CBS
phenol(donor)...water						
ΔE^{uncor}	−7.68	−7.31	−7.15	−7.62	−7.29	−7.15
ΔE^{cor}	−6.18	−6.56		−6.24	−6.57	
i-propanol(donor)···water						
ΔE^{uncor}	−5.66	−5.40	−5.29	−5.60	−5.39	−5.30
ΔE^{cor}	−4.45	−4.78		−4.51	−4.79	
i-propanol(acceptor)···$CH_3NH_3^+$[b]						
ΔE^{uncor}	−23.80	−23.55	−23.44	−23.66	−23.53	−23.48
ΔE^{cor}	−21.62	−22.54		−21.77	−22.55	
i-propanol(donor)···CH_3COO^-						
ΔE^{uncor}	−21.93	−21.53	−21.36	−21.80	−21.50	−21.37
ΔE^{cor}	−19.25	−20.17		−19.40	−20.20	
CH_3OH···oxocyclobutane[c]						
ΔE^{uncor}	−8.37	−7.80	−7.56	−8.25	−7.77	−7.57
ΔE^{cor}	−6.46	−6.86		−6.58	−6.88	
$CH_3NH_3^+$···oxocyclobutane[c]						
ΔE^{uncor}	−25.82	−25.58	−25.48	−25.74	−25.55	−25.47
ΔE^{cor}	−23.68	−24.46		−23.77	−24.47	
CH_3OH···oxocyclobutene[c]						
ΔE^{uncor}	−6.39	−5.99	−5.82			
ΔE^{cor}	−4.84	−5.17				
imidazole···oxocyclobutane[c]						
ΔE^{uncor}	−10.09	−9.27	−8.92			
ΔE^{cor}	−7.61	−7.97				
imidazole···i-propanol (acceptor)						
ΔE^{uncor}	−9.76	−8.95	−8.61			
ΔE^{cor}	−7.17	−7.66				
phenol(donor)···CH_3CONH_2						
ΔE^{uncor}	−14.05	−13.28	−12.96			
ΔE^{cor}	−10.81	−11.73				
CH_3GuaH^+···phenol (acceptor)						
ΔE^{uncor}	−18.29	−17.49	−17.15			
ΔE^{cor}	−15.35	−15.97				
phenol(donor)···CH_3COO^-						
ΔE^{uncor}	−29.34	−29.10	−29.01			
ΔE^{cor}	−26.62	−27.56				

[a] Energies in kcal/mol. Donor or acceptor role of i-propanol and phenol in the complexes are indicated. Geometries were optimized with the corresponding method using the aug-cc-pvdz or aug-cc-pvtz basis set. $\Delta E^{cor} = \Delta E^{uncor} - BSSE$. The complete basis set limit value, $\Delta E^{MP2}{}_{CBS}$, was estimated using eq 5. [b] Trans H−O−C−H moiety in i-propanol. [c] Aug-cc-pvtz values from ref 7.

experimentally derived structure. Our calculations with the aug-cc-pvtz basis set suggest that the O···O distance of about 2.86 Å is the more reliable separation.

MP2 Binding Energies. Hydrogen-bonding energies from non-CP optimizations at the MP2/aug-cc-pvtz and MP2/6-31+G* levels are summarized in Table 2, and for 12 complexes with the CBS limit in Table 5. The uncorrected and BSSE-corrected values were calculated according to eqs 2−4. The BSSE values and the geometry distortion energies (GEOM) from non-CP optimization are summarized in Table S1 of the Supporting Information.

The ΔE^{cor} values for i-propanol containing complexes in Table 2 are consistently more or less negative than the hydrogen-bond energies with a phenol partner, when the i-propanol is an acceptor or donor, respectively. This is in accord with the geometric results and indicates that for all of the studied complexes, the stronger hydrogen bond is accompanied by a smaller X···H separation, both at the MP2/aug-cc-pvtz and MP2/6-31+G* levels. Another observed trend is that the MP2/aug-cc-pvtz ΔE^{cor} values are more negative than their MP2/6-31+G* counterparts for the present series. In contrast, the ΔE^{uncor} values are more negative from calculations with the 6-31+G* compared to the aug-cc-pvtz basis set.

The ΔE^{cor} values in Table 2 may be assigned to three groups. On the MP2/aug-cc-pvtz level, the neutral complexes, the protonated, and anionic complexes fall in the energy ranges of −4.4 to −11.7, −16.0 to − 22.5, and −20.2 to −27.6 kcal/mol, respectively. Binding energies of the water complexes vary between −4.4 and −6.6 kcal/mol, depending on the partner molecule and whether the water molecule acts as a donor or acceptor throughout the bond formation. Corresponding to the general trend, water is most favorably a donor and an acceptor with i-propanol and phenol, respectively.

The alternative hydrogen-bonding energies (with reversed roles for the donor and the acceptor) are mostly different in complexes with phenol. In the water-phenol complexes, ΔE^{cor} varies within a range of 2 kcal/mol, and in the methanol and imidazole complexes the range is 3−4 kcal/mol. In contrast, ΔE^{cor} varies by up to 1.5 kcal/mol in the corresponding i-propanol complexes.

The asparagine/glutamine mimic, CH_3CONH_2, forms two hydrogen bonds with the hydroxy partner. ΔE^{cor} for the phenol complex is more negative by 1.6 kcal/mol than with an i-propanol partner. On the basis of the calculated bond lengths in Table 1, the ═O···H−O hydrogen bond seems to be the energy determining factor, and the trend for preference of a donor phenol is maintained only by this assumption. However, the energy effect of the N−H···O hydrogen bond formed in parallel may not be negligible. The hydrogen bonds in the complexes with CH_3CONH_2 are the most bent ones in the present series. By the assumption that the hydrogen bond is stronger when the X···H−Y bond angle is closer to being linear,

the bond angles of 135−142° in these complexes may be a consequence of the balance of forming one, nearly linear ═O···H−O bond, or two, largely bent hydrogen bonds.

For the protonated complexes, the absolute ΔE^{cor} values decrease in the $CH_3NH_3^+$, imidazoleH^+, CH_3GuaH^+ series. This effect is clearly seen in complexes with an acceptor phenol, where the energy range is 3.5 kcal/mol compared to 2.2 kcal/mol for complexes including i-propanol. In the anionic complexes with CH_3COO^-, the proton-donor preference of the phenol partner is revealed most clearly for the complexes in the present series. The difference in ΔE^{cor} is 7.4 kcal/mol, the largest for all corresponding pairs in Table 2. This $\Delta\Delta E^{cor}$ can come into existence despite a geometry distortion energy as much as 4.6 kcal/mol (see Table S1 in the Supporting Information).

The BSSE values (Table S1, corresponding also to $\Delta E^{uncor} - \Delta E^{cor}$) are −0.6 to −1.8, and −1.0 to −2.1 kcal/mol for the neutral and the ionic complexes, respectively. This corresponds to 10−20 and 5−10% of the respective ΔE^{uncor} values at the MP2/aug-cc-pvtz level. The BSSE/ΔE^{uncor} ratios are similar to those calculated for the complexes with cyclic ethers.[7] The BSSE values from MP2/6-31+G* calculations are in the range of −2.1 to −4.4 kcal/mol. Despite the considerably larger BSSE values with this smaller basis, the ΔE^{cor} values have been calculated to be consistent with the MP2/aug-cc-pvtz ΔE^{cor} values (see next section).

The geometric distortions (see Table S1 in the Supporting Information) are up to 2 kcal/mol at the MP2/aug-cc-pvtz level. The only exception, 4.6 kcal/mol for the $CH_3COO^-\cdots HO-C_6H_5$ (acetate···phenol) complex, indicates the readiness of the distortion of the components for reaching a strong hydrogen bond. Jeffrey assigned the strong hydrogen bond with an energy of 15−40 kcal/mol.[1b] Grabowski[1g] characterized the short strong hydrogen bond (SSHB) with further structural features such as an O···O distance of 2.40−2.55 Å,[31] a charge transfer of about 0.1−0.4 charge units, and an H···X distance being close to a covalent bond. For the acetate...phenol complex, ΔE^{cor} value is −27.6 kcal/mol, whereas the O−H bond stretches by more than 0.06 Å, and the system produces O···H and O···O distances of 1.49 and 2.52 Å, respectively. The Mulliken charge transfer from the acetate ion is 0.13 units, the CHELPG value is 0.14. Although the transferred Mulliken and CHELPG charges are close to the previous values, 0.12 and 0.10, respectively, for the CH_3COO^-···i-propanol complex, the O···O distance of 2.66 Å is considerably out of the preferred range.

Other systems, which may form strong hydrogen bonds, are the protonated complexes. The most negative ΔE^{cor} value of −22.54 kcal/mol was calculated for the $CH_3NH_3^+$···i-propanol complex. In this system, the N−H bond is stretched by 0.039 Å, and the N···O distance is 2.66 Å. The Mulliken and the CHELPG charge transfers are 0.12 and 0.11 charge units from the protonated partner. The N···O distance for the strong hydrogen bond is 2.5−2.6 Å.[1g,31] Thus, the present complex with its structural parameters may be on the verge of the group classification. The N...O distance in the $CH_3NH_3^+$···phenol complex is considerably larger with a value of 2.76 Å. In the imidazoleH^+···i-propanol complex, the N···O distance is again about 2.65 Å, but the binding energy is only 20.2 kcal/mol. Nonetheless, still remarkable 0.13 (Mulliken) and 0.09 (CHELPG) units of charge transfer were calculated for this system.

Table S2 in the Supporting Information summarizes the calculated changes in the zero-point energies, ΔZPE, at the MP2/6-31+G* level. The unscaled values vary between 0.8 and 2.2 kcal/mol. The largest values of 1.84−2.18 kcal/mol were calculated for the water complexes. Thus ΔZPE is large in these cases, regardless of whether the water molecule acts as a donor or an acceptor. For other complexes, ΔZPE is always larger in the corresponding pairs with a phenol compared to an i-propanol component. Overall, by considering the ΔZPE values of 1.3 and 0.8 kcal/mol, respectively, only the CH_3COO^-···phenol and the $CH_3NH_3^+$···i-propanol complexes may be considered as forming strong hydrogen bonds in the present series, according to the MP2/aug-cc-pvtz calculations.

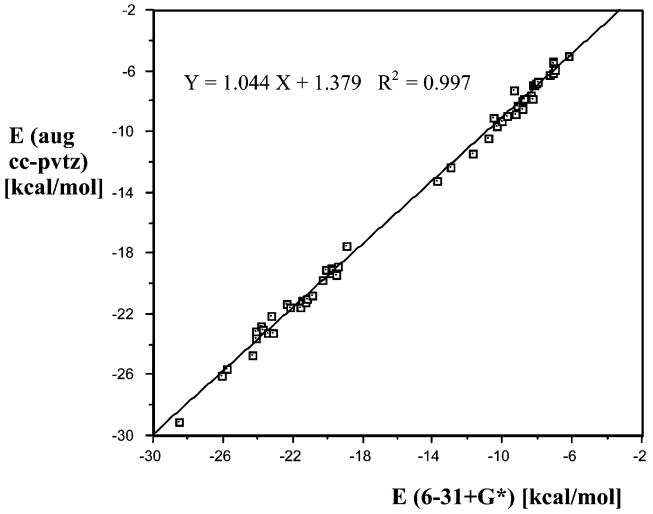

Figure 3. Correlation of the uncorrected MP2/6-31+G* and MP2/aug-cc-pvtz hydrogen-bonding energies for 28 neutral, 24 positively charged, and 2 negatively charged complexes in the gas phase. Energies in kcal/mol. See also Table 6.

The CBS limit is close to the aug-cc-pvtz uncorrected binding energy for each of the studied complexes. The CBS energy depends within a few hundredths of a kcal/mol on whether it was derived upon non-CP or CP optimization of the complex. This difference is, however, much smaller than that between the BSSE corrected and the CBS binding energy. If the extrapolation of the CBS value upon the application of eq 5 and the aug-cc-pvdz and aug-cc-pvtz binding energies is correct, then Table 5 suggests that the uncorrected aug-cc-pvtz binding energy is a much better estimation of the CBS limit than the BSSE-corrected value. However, this conclusion rests on considering only twelve hydrogen-bonded systems. Further studies and a larger variety of hydrogen-bonded complexes are necessary to explore whether the use of the aug-cc-pvtz uncorrected binding energy may provide a good estimation to the CBS limit value.

The correlation of the BSSE-uncorrected gas-phase hydrogen-bonding energies calculated at the MP2/6-31+G* and MP2/aug-cc-pvtz levels are shown in Figure 3. (For the correlation of the corrected binding energies, see Figure S1 in the Supporting Information.) The derived equations are summarized in Table 6. Correlation equations have been derived for a total of 54 complexes, 24 complexes from Table 2 and 30 complexes of amino acid mimics and cyclic ethers.[7] Separate equations were derived for the neutral and positively charged complexes (see also the footnote of Table 6). The two negatively charged complexes were only considered as part of the total set.

R^2 is equal to 0.997 and 0.996 for the uncorrected and corrected ΔE values, respectively. This indicates a good correlation of the corresponding MP2/aug-cc-pvtz and MP2/6-31+G* hydrogen-bonding energies for the total set. Neither Figure 3 nor Figure S1 in the Supporting Information show a remarkable outlier for the set of 54 complexes. The neutral and charged complexes appear in the −4 to −14 kcal and the −15

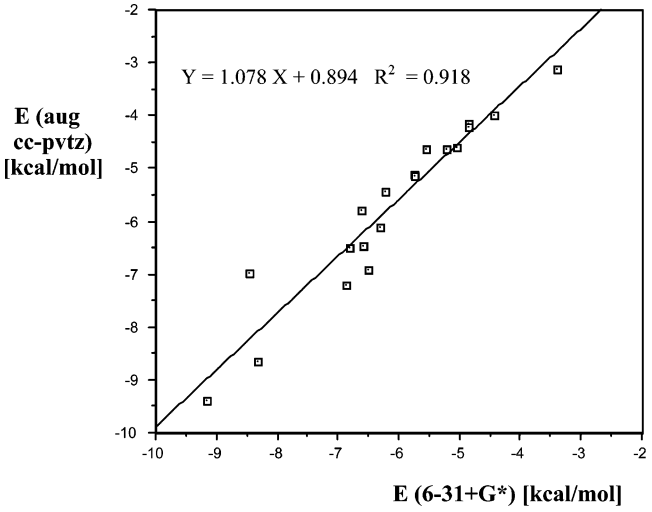

Figure 4. Correlation of the BSSE-uncorrected MP2/6-31+G* and MP2/aug-cc-pvtz hydrogen-bonding energies for 19 neutral complexes in a model continuum with dielectric constant of 15.0. Energies in kcal/mol. The plotted energies do not include contributions due to a cavity formation and dispersion−repulsion interactions throughout the hydrogen-bond formation. See also Table 6.

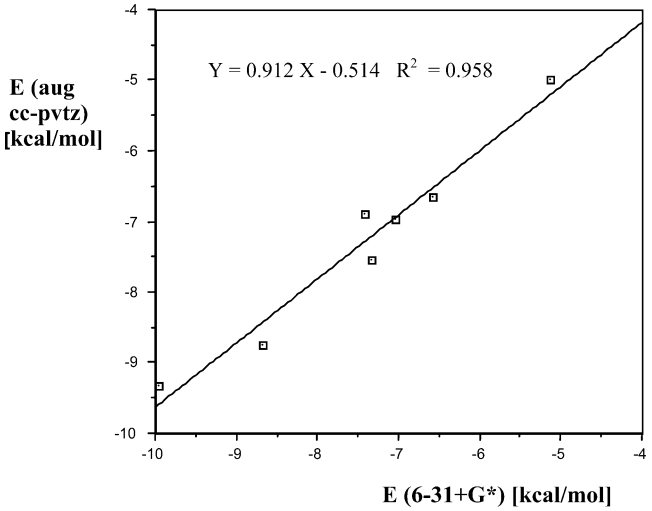

Figure 5. Correlation of the BSSE-uncorrected MP2/6-31+G* and MP2/aug-cc-pvtz hydrogen-bonding energies for 7 positively charged complexes in a model continuum. Energies in kcal/mol. See also Table 6 and the caption for Figure 4.

to −29 kcal/mol binding energy regions, respectively. Since these domains are not overlapping, it could be useful to develop separate equations for the neutral and charged species. Table 6 shows that the slopes are about 1.04 for the total set, but the average slope splits to 1.12−1.15 and 1.00−1.06 for the sets of the neutral and the positively charged complexes. A better estimation of the hydrogen-bond energy for a specific complex is expected if the group-specific correlation equation is applied.

The most important conclusion from Table 6 is that the MP2/aug-cc-pvtz binding energies in the gas-phase could be predicted on the basis of much simpler calculations at the MP2/6-31+G* level. Table 1 (and Table 4 in ref 7) show that the H..X distance for a specific hydrogen bond may differ by up to 0.1 Å, as calculated with the two basis sets. Nevertheless, the hydrogen-bond energies at the corresponding optimized geometries still correlate satisfactorily, both for the uncorrected and the BSSE corrected ΔE values.

The authors assume that eq 5 is an appropriate formula for predicting the CBS limit. Table 5 then shows that the uncorrected MP2/aug-cc-pvtz binding energy is more negative than the CBS limit by up to 0.35 kcal/mol in the gas phase for twelve complexes. A fairly easy prediction of the uncorrected MP2/aug-cc-pvtz binding energy at its non-CP optimized geometry could be beneficial in many practical applications. The present study suggests that the corresponding values could be predicted on the basis of non-CP MP2/6-31+G* geometry optimizations and binding energy calculations without applying the BSSE correction. This makes the calculation procedure at the MP2/6-31+G* level even shorter.

If future studies point out that the CBS estimation is not precise enough on the basis of eq 5, and the BSSE corrected energies turn out to be the theoretically more sound values for the binding energy even at the MP2/aug-cc-pvtz level, the correlation found in Table 6 for the BSSE corrected binding energies can still be applied, and calculations for everyday practice could then utilize the BSSE corrected MP2/6-31+G* binding energy values.

CCSD(T) Binding Energies. Eight complexes were selected for estimating the $\Delta E^{CCSD(T)}_{CBS}$ binding energies in the gas phase (Table 7). For the more affordable cases of the i-propanol···water and methanol···oxocyclobutene complexes, the $\Delta\Delta E = (\Delta E^{CCSD(T)} - \Delta E^{MP2})$ correction term was calculated both by using the aug-cc-pvdz and aug-cc-pvtz basis sets. For all complexes, the correction term was estimated both with and without the consideration of the basis-set superposition error.

$\Delta\Delta E$ differs only by a few hundredths of a kcal/mol when the aug-cc-pvdz or the aug-cc-pvtz basis set was used for either complex. Considering the BSSE uncorrected term, $\Delta\Delta E^{uncor}$, the $\Delta E^{CCSD(T)}_{CBS}$ value is more negative by −0.05 to −0.08 kcal/mol than the ΔE^{MP2}_{CBS} limit for the i-propanol···water complex. The correction is of opposite sign, but is very close to zero kcal/mol for the methanol···oxocyclobutene complex with the two basis sets. The difference of the $\Delta\Delta E^{cor}$ terms calculated with the two basis sets is slightly larger than the corresponding difference for the $\Delta\Delta E^{uncor}$ terms, but the largest difference is still less than 0.1 kcal. The two studied examples suggest that the $\Delta E^{CCSD(T)} - \Delta E^{MP2}$ correlation correction of the hydrogen-bonding energy may be reasonably estimated upon using the aug-cc-pvdz basis set without accounting for the basis set superposition error.

The largest calculated $\Delta\Delta E^{uncor}$ (aug-cc-pvdz) correction is 0.57 kcal/mol and the largest difference between the corresponding $\Delta\Delta E^{uncor}$ and $\Delta\Delta E^{cor}$ values is 0.16 kcal/mol. The correction terms assume both negative and positive values. Because the BSSE-uncorrected ΔE^{MP2}(aug-cc-pvtz) binding energies (referred to as ΔE^{MP2} in Table 7) were always more negative than the corresponding CBS limit in Table 5, the positive $\Delta\Delta E^{uncor}$ correction increases the difference between this value and $\Delta E^{CCSD(T)}_{CBS}$. Nonetheless, the overestimation of the $\Delta E^{CCSD(T)}_{CBS}$ binding energy by ΔE^{MP2} is generally up to 5 and 3% for the neutral and positively charged complexes, respectively. The overestimation is 11% only for the imidazole•••i-propanol complex. The number of the studied cases in Table 7 is far from forming a basis for generalization. The present results are, however, promising toward using the separate correlation equations for the neutral and protonated complexes (Table 6) and applying an empirical factor of about 0.95 and 0.97, respectively, such that the $\Delta E^{CCSD(T)}_{CBS}$ values in the gas phase may be estimated on the basis of BSSE uncorrected ΔE^{MP2}(6-31+G*) binding energies. Nonetheless, further calculations with special emphasis on the negatively charged systems are necessary for establishing a more solid empirical relationship.

TABLE 6. Correlations of the Uncorrected and BSSE Corrected Hydrogen-Bond Energies Calculated at the MP2/aug-cc-pvtz and MP2/6-31+G* Levels[a]

$Y = \Delta E^{uncor}$ (MP2/aug-cc-pvtz); ΔE^{cor} (MP2/aug-cc-pvtz)	$X = \Delta E^{uncor}$ (MP2/6-31+G*); ΔE^{cor} (MP2/6-31+G*)	
	Gas Phase	
total set, $n = 54$		
ΔE^{uncor}	$Y = 1.044X + 1.379$	$R^2 = 0.997$
ΔE^{cor}	$Y = 1.040X - 0.558$	$R^2 = 0.996$
neutral complexes, $n = 28$		
ΔE^{uncor}	$Y = 1.120X + 2.000$	$R^2 = 0.969$
ΔE^{cor}	$Y = 1.146X + 0.067$	$R^2 = 0.956$
positively charged complexes, $n = 24$		
ΔE^{uncor}	$Y = 1.060X + 1.837$	$R^2 = 0.964$
ΔE^{cor}	$Y = 0.996X - 1.324$	$R^2 = 0.971$
	In Environment	
total set, $n = 28$		
ΔE^{uncor}	$Y = 1.125X + 1.077$	$R^2 = 0.929$
neutral complexes, $n = 19$		
ΔE^{uncor}	$Y = 1.078X + 0.894$	$R^2 = 0.918$
positively charged complexes, $n = 7$		
ΔE^{uncor}	$Y = 0.912X - 0.514$	$R^2 = 0.958$

[a] Energies in kcal/mol. The total set in the gas phase includes 24 complexes from Table 2, and 30 complexes of amino acid mimics and cyclic ethers from ref 7, Table 5. Neutral complexes: 16 from the present study + 12 ether complexes. Positively charged complexes: 6 from the present study + 18 ether complexes. For the in-environment correlations, complexes were considered in Tables 9 and 10.

TABLE 7. Complete Basis Set CCSD(T) Binding Energies for Selected Gas-phase Complexes[a]

		$\Delta\Delta E = \Delta E^{CCSD(T)} - \Delta E^{MP2}$				
		aug-cc-pvdz		aug-cc-pvtz		
	ΔE^{MP2b}	$\Delta\Delta E^{uncor}$	$\Delta\Delta E^{cor}$	$\Delta\Delta E^{uncor}$	$\Delta\Delta E^{cor}$	$\Delta E^{CCSD(T)}$CBS
i-propanol···water	−5.40	−0.08	−0.01	−0.05	−0.06	−5.37 (−5.34)
CH_3OH···oxocyclobutene	−5.99	−0.02	0.07	0.03	0.00	−5.84 (−5.79)
imidazole···i-propanol	−8.95	0.57	0.64			−8.04
phenol···CH_3CONH_2	−13.28	0.29	0.45			−12.67
CH_3GuaH^+···phenol	−17.49	0.15	0.28			−17.00
i-propanol···CH_3COO^-	−21.53	−0.15	−0.01			−21.51
$CH_3NH_3^+$···i-propanol[c]	−23.55	0.42	0.48			−23.02
phenol···CH_3COO^-	−29.10	0.49	0.64			−28.52

[a] Energies in kcal/mol. The first standing partner is the hydrogen-bond donor for the complexes in the table. The complete basis set limit values, $\Delta E^{CCSD(T)}{}_{CBS}$, were calculated by utilizing the $\Delta E^{MP2}{}_{CBS}$ values (Table 5) and the $\Delta\Delta E = \Delta E^{CCSD(T)} - \Delta E^{MP2}$ energy difference. Values in parentheses were obtained by considering the aug-cc-pvtz $\Delta\Delta E^{uncor}$ terms. [b] For comparison, ΔE^{uncor} (MP2/aug-cc-pvtz) values calculated with non-CP optimization (Table 5). [c] Trans H−O−C−H moiety in i-propanol.

In-Environment Calculations. The changes in the binding energies for all 24 complexes under the influence of a polarizable environment were estimated throughout the IEF-PCM approximation at the MP2 level, utilizing the gas-phase optimized geometries (Table 8). Upon these single-point calculations, the effect of the environment on the equilibrium geometry was discarded, and the comparison of the gas-phase and in-environment (condensed-phase) values directly account for the polarization effect of the model environment with a dielectric constant of $\epsilon = 15.0$. Because the implementation of the IEF-PCM method in Gaussian 03 does not allow for the calculation of the BSSE correction, the following discussion compares the ΔE^{uncor} values calculated in the two phases.

All individual E_{elst} terms, for either the components or the hydrogen-bonded dimers (data not shown), were calculated at negative values. Thus the electrostatic interaction is favorable for the molecules under consideration when they enter a polarizable environment from the gas phase. The ΔE_{elst} term following the hydrogen-bond formation was, however, always calculated as providing a positive-energy contribution. Table 8 shows the breakdown of the total condensed-phase ΔE^{uncor} to ΔE_{elst} and $\Delta(E_{int} + E_2)$. E_{int} was calculated according to eq 6a and E_2 is the second-order Moller−Plesset (MP2) energy correction to the internal energy.

$\Delta(E_{int} + E_2)$ is always more negative than its gas-phase counterpart, ΔE^{uncor}(gas), which corresponds to ΔE^{uncor} itself in the gas phase. In contrast, due to a considerably positive ΔE_{elst} component, the electrostatic part of the binding energy in the condensed phase, defined as $\Delta E^{uncor}(cp) = \Delta E_{elst} + \Delta(E_{int} + E_2)$, has been calculated always less negative than the ΔE^{uncor}(gas) value. It is to be emphasized, however, that the above definition of the condensed-phase ΔE^{uncor} does not account either for the energy possibly needed for covering a cavity formation in the protein environment or due to the changes in the dispersion−repulsion interaction free energies throughout the hydrogen bond formation.

The most important changes for $\Delta E^{uncor}(cp)$ have been calculated for the ionic hydrogen bonds. In these cases, the ΔE_{elst} terms are as large as 10.4−17.5 kcal/mol. As a consequence, the uncorrected MP2/aug-cc-pvtz binding energies decrease (in absolute value) from the range of −17.5 to −29.1 kcal/mol in the gas phase to the range of −5.0 to −11.4 kcal/mol. It is also noticeable that for the positively charged systems, the largest and smallest stabilities of the $CH_3NH_3^+$ and CH_3GuaH^+ complexes, respectively, switch when they enter from the gas-phase in a polarizable environment with $\epsilon = 15.0$. The changes calculated for the neutral complexes are smaller, but ΔE^{uncor} is still less negative by 1−5 kcal/mol in the condensed phase than

TABLE 8. Uncorrected Binding Energies from Ab Initio MP2/aug-cc-pvtz and MP2/6-31+G* Calculations in a Model Continuum Environment with a Dielectric Constant of 15.0[a]

	i-propanol (acceptor)			phenol(acceptor)		
	ΔE_{elst}	$\Delta(E_{int}+E_2)$	ΔE^{uncor}	ΔE_{elst}	$\Delta(E_{int}+E_2)$	ΔE^{uncor}
CH_3OH	2.86	−7.91	−5.05[b]	1.81	−6.46	−4.65
	3.25	−8.97	−5.72[b]	1.73	−7.28	−5.55
imidazole	3.34	−9.80	−6.46	3.09	−9.20	−6.11
	3.95	−10.55	−6.60	3.72	−10.03	−6.31
$CH_3NH_3^+$	16.77	−23.84	−7.07[b]	15.81	−20.81	−5.00
	16.91	−24.01	−7.10[b]	14.35	−19.49	−5.14
imidazoleH^+	13.18	−21.92	−8.74	13.82	−20.48	−6.66
	13.72	−22.40	−8.68	14.35	−20.94	−6.59
CH_3GuaH^+	12.45	−21.77	−9.32	10.41	−17.29	−6.88
	12.64	−22.59	−9.95	11.39	−18.80	−7.41
water	3.09	−7.70	−4.61	3.03	−6.17	−3.14
	3.58	−8.64	−5.06	3.06	−6.46	−3.40
	3.03	−7.68	−4.65[b]			
	3.53	−8.74	−5.21[b]			

	i-propanol (donor)			phenol(donor)		
	ΔE_{elst}	$\Delta(E_{int}+E_2)$	ΔE^{uncor}	ΔE_{elst}	$\Delta(E_{int}+E_2)$	ΔE^{uncor}
CH_3OH	2.11	−7.23	−5.12	2.78	−9.76	−6.98
	2.62	−8.37	−5.75	2.04	−10.51	−8.47
imidazole	2.68	−10.14	−7.46[b]	4.17	−13.56	−9.39
	3.48	−10.69	−7.21[b]	4.99	−14.16	−9.17
CH_3CONH_2	6.07	−12.97	−6.90	6.42	−15.06	−8.64
	6.68	−13.18	−6.50	7.13	−15.45	−8.32
CH_3COO^-	15.13	−22.57	−7.44	17.45	−28.89	−11.44
	15.57	−22.36	−6.79	17.66	−27.89	−10.23
water	1.89	−6.05	−4.16	2.29	−8.09	−5.80
	2.59	−7.46	−4.85	3.13	−9.75	−6.62
	1.90	−6.11	−4.21[b]			
	2.58	−7.42	−4.84[b]			

[a] Energies in kcal/mol. Single-point in-environment calculations at the gas-phase optimized geometries. ΔE_{elst} and ΔE_{int} from eqs 6a and 6b, respectively. E_2 is the second-order Moller−Plesset correction to the internal energy. Upper and lower values from MP2/aug-cc-pvtz and MP2/6-31+G* calculations, respectively. The H−O−C−H moiety is in gauche conformation in i-propanol, with the exception of the indicated water complexes, where the conformation is trans. [b] Trans H−O−C−H moiety in i-propanol.

in the gas phase. Similar conclusions are valid for the studied four complexes with cyclic ether acceptors (Table 9).

The $\Delta E^{CCSD(T)}{}_{CBS}$ values were calculated for four selected complexes representing different classes of the hydrogen-bonded complexes: neutral, or ionic with a +1 or −1 net charge (Table 10). The basic conclusion is that the polarizable environment does not change the $(\Delta E^{CCSD(T)} - \Delta E^{MP2})$ correction term remarkably when compared to that for the gas phase. Thus, this correction may be calculated from the computationally less demanding gas-phase models.

Table 6 includes the correlation equations between the 6-31+G* and aug-cc-pvtz ΔE^{uncor} values in the model environment. The R^2 values are smaller than in the case of the gas-phase binding energies, but still allow a useful prediction of high-level binding energies on the basis of MP2/6-31+G* calculations in a polarizable dielectric. Considering a total of 28 complexes (see Figure S2 in the Supporting Information), the R^2 value is 0.929. As for the gas-phase complexes, separate correlation equations would allow a better prediction of the specific type of the hydrogen-bond energy. The correlation is remarkably better when only the positive ions are considered, and only slightly worsen for the neutral species (Figures 4 and 5). The intercepts are much different for the positive ions and the neutral molecules, thus the use of individual correlation equations is justified. Good prediction of the ionic hydrogen-bond energies is crucial for calculating a correct net binding energy with several binding sites. ΔE^{uncor} for ionic hydrogen bonds provide generally larger contributions to the total binding energies than the neutral ones, and thus such complexes have to draw large interest. In the present study, only two negatively charged complexes have been investigated. Our future work targets calculations in this field, studying the CH_3-COO^- complexes with hydrogen-bond donor amino acid mimics such as $CH_3NH_3^+$, CH_3GuaH^+, CH_3CONH_2, and neutral and protonated imidazole. These complexes may model internal hydrogen bonds and salt-bridges in proteins. Such model calculations augmented with the acetate···water complex could provide a basis for establishing a correlation equation for complexes including the $-COO^-$ group as an acceptor.

Conclusions

The hydrogen-bonding energy was calculated for 24 pairs of complexes comprised of isopropyl alcohol (i-propanol) and phenol as one partner, and water and amino-acid mimics (methanol, acetamide, neutral and protonated imidazole, protonated methylalamine, the methyl-guanidium cation, and the

TABLE 9. Uncorrected Binding Energies for Cyclic-Ether-Containing Hydrogen-Bonded Complexes in a Model Continuum Environment with a Dielectric Constant of 15.0[a]

	MP2/aug-cc-pvtz			MP2/6-31+G*		
	ΔE_{elst}	$\Delta(E_{int}+E_2)$	ΔE^{uncor}	ΔE_{elst}	$\Delta(E_{int}+E_2)$	ΔE^{uncor}
CH_3OH···oxocyclobutene	2.68	−6.66 (−5.99)[b]	−3.98	3.14	−7.57 (−6.99)	−4.43
CH_3OH···oxocyclobutane	3.23	−8.66 (−7.80)	−5.43	3.27	−9.50 (−8.80)	−6.23
$CH_3NH_3^+$···oxocyclobutane	18.97	−26.53 (−25.58)	−7.55	19.37	−26.70 (−25.81)	−7.33
imidazole···oxocyclobutane	3.83	−10.34 (−9.27)	−6.51	4.38	−11.19 (−10.05)	−6.81

[a] Energies in kcal/mol. Single-point in-environment calculations at the gas-phase optimized geometries. See also the footnote for Table 8. [b] Values in parentheses stand for the gas-phase uncorrected binding energies from ref 7.

TABLE 10. Complete Basis Set CCSD(T) Binding Energies for Selected Complexes in a Model Continuum Environment with a Dielectric Constant of 15.0[a]

	ΔE^{MP2}[b]	$\Delta E^{MP2}{}_{CBS}$	$(\Delta E^{CCSD(T)} - \Delta E^{MP2})$[c]	$\Delta E^{CCSD(T)}{}_{CBS}$[d]
phenol···water	−5.80	−5.64	−0.06	−5.70
CH_3OH···oxocyclobutene	−3.98	−3.75	−0.08	−3.83
i-propanol···CH_3COO^-	−7.44	−7.24	−0.16	−7.40
$CH_3NH_3^+$···i-propanol[e]	−7.07	−6.93	0.30	−6.63

[a] Energies in kcal/mol. Single-point in-environment calculations at the gas-phase optimized geometries. The first standing partner is the hydrogen-bond donor for the complexes in the table. [b] ΔE(MP2/aug-cc-pvtz) binding energies in the condensed phase without BSSE correction (ΔE^{uncor}). [c] BSSE-uncorrected aug-cc-pvdz values for the $(\Delta E^{CCSD(T)} - \Delta E^{MP2})$ energy difference. [d] The complete basis set limit values were calculated according to eq 1. [e] Trans H−O−C−H moiety in i-propanol.

acetate anion) as the other partner. Molecular geometries were optimized and zero-point-energies were determined at the MP2/6-31+G* level. All structures were reoptimized at the MP2/aug-cc-pvtz level. The X···H distances and X···H−Y bond angles differed by up to about 0.1 Å and 6°, respectively, with the two basis sets.

The BSSE values from the Boys−Bernardi counterpoise calculations amount to 10−20 and 5−10% of the uncorrected binding energies of the neutral and ionic complexes, respectively, at the MP2/aug-cc-pvtz level. These fractions of energies are very similar to those calculated by us previously for complexes between cyclic ethers and amino-acid mimcs.[7] The geometry distortion energy upon hydrogen-bond formation is up to 2 kcal/mol, with the exception of the most strongly bound acetate...phenol complex, where the GEOM term reached a value of 4.6 kcal/mol.

On the basis of the X···Y heavy atom and X···H distances, as well as by considering the CHELPG charge transfer from the acceptor to the donor molecule, the $CH_3COO^-\cdots HO-C_6H_5$ (acetate···phenol) system with BSSE-corrected binding energy of −27.56 kcal/mol has been classified as a short, strong hydrogen bond (SSHB) in the gas phase.[1g] The $CH_3NH_3^+\cdots$ isopropyl alcohol complex with binding energy of −22.54 kcal/mol is on the verge of this classification.

The CBS limit of the binding energy in the gas phase has been calculated for twelve and six complexes with non-CP and CP geometry optimizations, respectively. Although the X···Y distances of the X−H···Y bridges differ by up to 0.03 Å, the difference in the derived CBS values is only up to 0.03 kcal/mol. The uncorrected MP2/aug-cc-pvtz hydrogen-bonding energies differ by up to 0.35 kcal/mol for the studied complexes including seven neutral and five charged species. The CCSD(T)$_{CBS}$ binding energies in the gas phase differ from the uncorrected MP2/aug-cc-pvtz values generally by up to 5% for the neutral, and up to 3% for the ionic hydrogen bonds.

A polarizable environment largely modifies the hydrogen-bonding energies. In a model continuum with $\epsilon = 15.0$, the uncorrected MP2/aug-cc-pvtz binding energies decreased (in absolute value) by 11−18 kcal/mol for the nine ionic species and by up to 5 kcal/mol for the nineteen neutral complexes, without considering possibly necessary cavity formations in a protein environment and dispersion-repulsion related energy changes. The $\Delta E^{CCSD(T)} - \Delta E^{MP2}$ correction added to the $\Delta E^{MP2}{}_{CBS}$ value for estimating the CBS limit of the $\Delta E^{CCSD(T)}$ binding energy in a model environment is similar to the corresponding value in the gas phase for the studied two neutral, one positively and one negatively charged hydrogen-bonded complexes.

The gas-phase MP2/aug-cc-pvtz hydrogen-bonding energies correlate well ($R^2 = 0.997$) with the corresponding MP2/6-31+G* values facilitating the prediction of the uncorrected MP2/aug-cc-pvtz hydrogen-bonding energies, near the CBS limit, on the basis of much simpler MP2/6-31+G* calculations. If the effect of the polarizable environment is also considered, the correlation coefficient reduced to $R^2 = 0.929$ for 28 species. Still, this correlation is capable of estimating the condensed-phase $\Delta E^{CCSD(T)}{}_{CBS}$ binding energies for the most studied complexes at a precision of about 1 kcal/mol on the basis of MP2/6-31+G* calculations.

Acknowledgment. The authors thank the Ohio Supercomputer Center for the granted computer time. The USDA grant support provided to P.E. is also acknowledged.

Supporting Information Available: The BSSE and GEOM values from ab initio MP2/aug-cc-pvtz and MP2/6-31+G* calculations and the MP2/6-31+G* zero-point-energies for 24 complexes (Tables S1 and S2), the plot of the BSSE-corrected gas-phase MP2/aug-cc-pvtz binding energies vs the MP2/6-31+G* values (Figure S1), and the plot of the BSSE-uncorrected MP2/aug-cc-pvtz binding energies vs the MP2/6-31+G* values in a model continuum with dielectric constant of 15.0 (PDF). This material is available free of charge via Internet at http://pubs.acs.org.

References and Notes

(1) See e.g. (a) *Modeling the Hydrogen Bond*; Smith, D. A., Ed.; ACS Symposium Series 569; American Chemical Society, Washington D.C., 1994. (b) *An Introduction to Hydrogen Bonding*; Jeffrey, G. A., Ed.; Oxford University Press: New York, 1997. (c) Scheiner, S. *Hydrogen Bonding: A Theoretical Perspective*; Oxford University Press, New York, 1997. (d) Desiraju, G.; Steiner, T. *The Weak Hydrogen Bond: Applications to Structural Chemistry and Biology*; Oxford University Press: New York, 1999. (e) *Horizons in Hydrogen Bond Research 2003* In *J. Mol. Struct.* **2004**, *700* (1−3); Barnes, A. J.; Limbach, H.-H., Eds.; Elsevier B. V.: Amsterdam, 2004. (f) Hobza, P. *Annu. Rep. Prog. Chem., Sect. C* **2004**, *100*, 3. (g) Grabowski, S. J. *Annu. Rep. Prog. Chem., Sect. C* **2006**, *102*, 131. (h) Marx, D. *ChemPhysChem*. **2006**, *7*, 1848.

(2) Keasling, H.; Schueler, F. *J. Am. Pharm. Assoc.* **1950**, *39*, 87.

(3) Tanenbaum, D. M.; Wang, Y.; Williams, S. P.; Sigler, P. B. *Proc. Natl. Acad. Sci. U.S.A.* **1998**, *95*, 5998.

(4) Kavlock, R. J.; Daston, G. P.; DeRosa, C.; Fenner-Crisp, P.; Gray, L. E.; Kaattari, S.; Lucier, G.; Luster, M.; Mac, M. J.; Maczka, C.; Miller, R.; Moore, J.; Rolland, R.; Scott, G.; Sheehan, D. M.; Sinks, T.; Tilson, H. A. *Environ. Health Perspect.* **1996**, *104* (Suppl. 4), 715.

(5) Dixon, R. A.; Ferreira, D. *Phytochemistry* **2002**, *60*, 205.

(6) Matsumura, A.; Ghosh, A.; Pope, G. S.; Darbre, P. D. *J. Steroid Biochem. Mol. Biol.* **2005**, *94*, 431.

(7) Nagy, P. I.; Erhardt, P. W. *J. Phys. Chem. A* **2006**, *110*, 13923.

(8) Hehre, W. J.; Radom, L.; Schleyer, P. v. R.; Pople, J. A. *Ab Initio Molecular Orbital Theory*; Wiley: New York, 1986.

(9) (a) Møller, C.; Plesset, M. S. *Phys. Rev.* **1934**, *46*, 618. (b) Pople, J. A.; Binkley, J. S.; Seeger, R. *Int. J. Quantum Chem.* **1976**, *10s*, 1. (c) Krishnan, R.; Frisch, M. J.; Pople, J. A. *J. Chem. Phys.* **1980**, *72*, 4244. (d) Pople, J. A.; Head-Gordon, M.; Raghavachari, K. *J. Chem. Phys.* **1987**, *87*, 5968.

(10) (a) Kendall, R. A.; Dunning, T. H., Jr.; Harrison, R. J. *J. Chem. Phys.* **1992**, *96*, 6796. (b) For a recent review on the correlation-consistent basis sets, see Peterson, K. A. *Annu. Rep. Comput. Chem.* **2007**, *3*, 195.

(11) van Duijneveldt, F. B.; van Duijneveldt-van de Rijdt, J. G. C. M.; van Lenthe, J. H. *Chem. Rev.* **1994**, *94*, 1873.

(12) Boys, S. F.; Bernardi, F. *Mol. Phys.* **1970**, *19*, 553.

(13) Nagy, P. I.; Smith, D. A.; Alagona, G.; Ghio, C. *J. Phys. Chem.* **1994**, *98*, 486.

(14) Smit, P. H.; Derissen, J. L.; van Duijneveldt, F. B. *J. Chem. Phys.* **1978**, *69*, 4241.

(15) Simon, S.; Duran, M.; Dannenberg, J. J. *J. Chem. Phys.* **1996**, *105*, 11024.

(16) Hobza, P.; Havlas, Z. *Theor. Chem. Accounts* **1998**, *99*, 372.

(17) Halkier, A.; Koch, H.; Jorgensen, P.; Christiansen, O.; Beck Nielsen, I. M.; Helgaker, T. *Theor. Chem. Accounts* **1997**, *97*, 150.

(18) (a) Wilson, A.; Dunning, T. H., Jr. *J. Chem. Phys.* **1997**, *106*, 8718. (b) Helgaker, T.; Klopper, W.; Koch, H.; Noga, J. *J. Chem. Phys.* **1997**, *106*, 9639.

(19) Grabowski, S. J.; Sokalski, W. A.; Leszczynski, J. *J. Phys. Chem. A* **2005**, *109*, 4331.

(20) Raghavachari, K.; Trucks, G. W.; Pople, J. A.; Head-Gordon, M. *Chem. Phys. Lett.* **1989**, *157*, 479.

(21) Breneman, C. M.; Wiberg, K. B. *J. Comput. Chem.* **1990**, *11*, 361.

(22) *Sybyl*, version 7.1; Tripos Inc.; St. Louis, MO, 2005.

(23) (a) Miertus, S.; Scrocco, E.; Tomasi, J. *Chem. Phys.* **1981**, *55*, 117. (b) Tomasi, J.; Persico, M. *Chem. Rev.* **1994**, *94*, 2027. (c) Cramer, C. J.; Truhlar, D. G. *Chem. Rev.* **1999**, *99*, 2161. (d) Orozco, M.; Luque, F. J. *Chem. Rev.* **2000**, *100*, 4187. (f) Tomasi, J.; Mennucci, B.; Cammi, R. *Chem. Rev.* **2005**, *105*, 2999.

(24) (a) Cancès, E.; Mennucci, B.; Tomasi, J. *J. Chem. Phys.* **1997**, *107*, 3032. (b) Cancès, E.; Mennucci, B. *J. Chem. Phys.* **1998**, *109*, 249. (c) Cancès, E.; Mennucci, B. *J. Chem. Phys.* **1998**, *109*, 260.

(25) Bondi, A. *J. Phys. Chem.* **1964**, *68*, 441.

(26) Nagy, P. I.; Alagona, G.; Ghio, C. *J. Chem. Theory Comput.* **2007**, *3*, 1249.

(27) Frisch, M. J.; Trucks, G. W.; Schlegel, H. B.; Scuseria, G. E.; Robb, M. A.; Cheeseman, J. R.; Montgomery, J. A., Jr.; Vreven, T.; Kudin, K.

N.; Burant, J. C.; Millam, J. M.; Iyengar, S. S.; Tomasi, J.; Barone, V.; Mennucci, B.; Cossi, M.; Scalmani, G.; Rega, N.; Petersson, G. A.; Nakatsuji, H.; Hada, M.; Ehara, M.; Toyota, K.; Fukuda, R.; Hasegawa, J.; Ishida, M.; Nakajima, T.; Honda, Y.; Kitao, O.; Nakai, H.; Klene, M.; Li, X.; Knox, J. E.; Hratchian, H. P.; Cross, J. B.; Bakken, V.; Adamo, C.; Jaramillo, J.; Gomperts, R.; Stratmann, R. E.; Yazyev, O.; Austin, A. J.; Cammi, R.; Pomelli, C.; Ochterski, J. W.; Ayala, P. Y.; Morokuma, K.; Voth, G. A.; Salvador, P.; Dannenberg, J. J.; Zakrzewski, V. G.; Dapprich, S.; Daniels, A. D.; Strain, M. C.; Farkas, O.; Malick, D. K.; Rabuck, A. D.; Raghavachari, K.; Foresman, J. B.; Ortiz, J. V.; Cui, Q.; Baboul, A. G.; Clifford, S.; Cioslowski, J.; Stefanov, B. B.; Liu, G.; Liashenko, A.; Piskorz, P.; Komaromi, I.; Martin, R. L.; Fox, D. J.; Keith, T.; Al-Laham, M. A.; Peng, C. Y.; Nanayakkara, A.; Challacombe, M.; Gill, P. M. W.; Johnson, B.; Chen, W.; Wong, M. W.; Gonzalez, C.; Pople, J. A. *Gaussian 03*, Revision C.02; Gaussian, Inc.; Wallingford, CT, 2004.

(28) (a) Gerhards, M.; Schmitt, M.; Kleinermanns, K.; Stahl, W. *J. Chem. Phys.* **1996**, *104*, 967. (b) Berden, G.; Meerts, W. L.; Schmitt, M.; Kleinermanns, K. *J. Chem. Phys.* **1996**, *104*, 972.

(29) Larsen, N. W. *J. Mol. Struct.* **1979**, *51*, 175.

(30) Benedict, W. S.; Gailar, N.; Plyler, E. K. *J. Chem. Phys.* **1956**, *24*, 1139.

(31) Frey, P. A. *Magn. Reson. Chem.* **2001**, *39*, 190.